Astron. Astrophys. 189, 232–242 (1988)

ASTRONOMY
AND
ASTROPHYSICS

A two-component working model for the atmosphere of a large sunspot umbra

V.N. Obridko[1] **and J. Staude**[2]

[1] Institute of Terrestrial Magnetism, Ionosphere and Radio Wave Propagation (IZMIRAN) of the USSR Academy of Sciences, SU-142092 Moscow-Troitsk, USSR
[2] Zentralinstitut für Astrophysik, Sonnenobservatorium Einsteinturm, DDR-1560 Potsdam, GDR

Received May 6, 1986; accepted May 18, 1987

Summary. A two-component working model has been proposed for the atmosphere of the umbra of a 'typical' large sunspot. The main component consists of cold matter at photospheric levels, a thin chromosphere, a shallow transition region, and a deep-set corona. The secondary component is assumed to have a volume filling factor of $\beta \approx 5$ to 10% at all heights and to consist of thin fine structure elements which are elongated parallel to the magnetic field; this matter should be hot at photospheric levels (bright dots), it should have a more extended chromosphere and relatively cold elements at higher levels, that is an amply extended, almost isothermal transition region at heights where the main component already reaches coronal temperatures. The filling factor seems to increase in 'active' phases of the spot's development (light bridges, EUV plumes); in such phases the pressure in the transition region of the secondary component is three times larger than quiescent values.

The two components of the umbral working model and an average quiet sun model for reference are based on uniform physical assumptions at all heights of a common geometrical height scale. The model represents an improvement of the earlier 'Wroclaw-Ondrejov sunspot model' and is able to explain basic features of sunspot observations at various frequencies from X-rays up to microwaves. The basic hypothesis of a direct connection between fine structures in the umbral photosphere and the transition region should be verified by further observations.

Key words: sunspot umbra – photosphere – chromosphere – corona

1. Introduction

Sunspots are the strongest concentrations of magnetic flux in the solar atmosphere and the kernels of solar active regions. The investigation of the basic physical processes and structures in the atmosphere such as mechanical and energy balance, stability, waves and oscillations, suggests the derivation of a semi-empirical model as a first step. Such a model should describe the spatial distribution of thermodynamic quantities over a large range of heights in the umbral atmosphere, from the deepest photospheric layers up to the lower corona above the spot. The model should be able to explain as many different observations as possible, including intensities from soft X-rays up to microwaves. Of course, each sunspot is an individual with its own structure and development, and ideally the model should be derived for one special sunspot at one phase of its development. Unfortunately, not all of the necessary data are available for such a situation, and we are forced to work up observed data from different sunspots into a model of a typical large sunspot umbra in a stable phase of its development.

Many efforts have been made to derive semi-empirical sunspot models; a comprehensive review has been given in a book recently published by one of the present authors (Obridko, 1985), and details will not be repeated here. Most of those models were restricted to a narrow range of heights in each case, but different physical assumptions render it difficult to combine several models relating to separate heights. Inhomogeneities have been ignored in most cases, although evidence for fine structures in sunspot umbrae has been given more than a century ago.

In the present paper we shall try to derive an umbral working model extending from photospheric up to coronal levels and assuming a two-component approximation to consider fine structures at all heights. In the next section some earlier approaches of modelling and the basic features of the present attempt will be outlined. In the subsequent chapters we shall represent the proposed model at photospheric and chromospheric heights (Sect. 3.1), in the transition region and lower corona (Sect. 3.2), and finally possible improvements and applications will be discussed (Sect. 4).

2. Some steps towards a unified umbral working model

A horizontally averaged working model for the umbra of a large stable sunspot has been proposed by one of the present authors (Staude, 1981). This model was based on uniform and self-consistent physical assumptions for all layers, including the photosphere (here the model practically agreed with that of Stellmacher and Wiehr, 1975), the lower chromosphere up to temperatures of $T \leq 1.1\,10^4$ K (in agreement with Teplitskaya et al., 1978), and the upper chromosphere up to temperatures of $T \leq 4.2\,10^4$ K (derived from EUV data with high spatial resolution). The model was able to explain the basic features of many observations at different wavelengths, including latest data from space. The chromospheric part of the umbral model strongly differed from earlier

Send offprint requests to: J. Staude

published models, especially a steeper gradient of $T(z)$ (z is the geometrical height) was necessary in order to explain the observed intensities of EUV lines by sufficiently large densities in a hydrostatic model. Lites and Skumanich (1981, 1982) derived a chromospheric umbral model the average $T(z)$ of which is similar to that in the model of Staude (1981; for a comparison of both models see Staude et al., 1983); the same $T(z)$ has also been adapted by Avrett (1981) to calculate the Sunspot sunspot model. The models differ from each other by the assumption of two plateaus of temperature at $T \approx 7000$ K and 23000 K in the Lites and Skumanich model, while a steady gradient of $T(z)$ has been proposed by Staude (1981). Either of the two types of models has some advantages in explaining special observed features, e.g., a plateau model results in ratios of peak intensities in the Ca II H/K and Mg II h/k lines which are closer to the observed ones, but the weak or missing central self-severals in such resonance lines (Lites and Skumanich, 1982; Gurman, 1984) and the frequency spectrum of umbral chromospheric oscillations (Staude et al., 1985) are easier explained by a gradient model.

The model of Staude (1981) has been adapted as the lower (photospheric and chromospheric) part of a benchmark model for a larger range of heights in the atmosphere above a large sunspot umbra. This "Wroclaw-Ondřejov sunspot model" (hereafter, WOSM, Staude et al., 1983, 1984) assumes a two-component structure in the chromosphere-corona transition region (TR) and in the lower corona: A hot main component has a shallow TR and deep-set corona, that means values of $T \approx 1.8\,10^6$ K and electron density $n_e \approx 10^9\,\mathrm{cm}^{-3}$ at $z \approx 3000$ to 5000 km above the umbral photosphere. A secondary component with a filling factor of $\beta \approx 0.1$ consists of comparatively cold filaments with an extended TR. Only such an inhomogeneous model is able to explain the majority of emissions observed in the upper layers of the umbral atmosphere: The bulk of microwave emission with brightness temperatures around $1.8\,10^6$ K and strong polarization is produced by gyromagnetic emission in the main component which is also responsible for the low intensity in soft X-ray lines, but the EUV lines are mainly formed in the secondary component of the WOSM.

It has already been mentioned that there is evidence for fine structures in the umbral photosphere as well: Each umbra seems to consist of a dark main component enclosing a large number of bright dots which cover the whole umbral area, similar to the usual granulation in the undisturbed photosphere (Bumba et al., 1975; Loughhead et al., 1979). The umbral dots have been tentatively explained by a reflection of convection in deeper umbral layers (Obridko, 1974a; Parker, 1979), by a residual cellular convection modified by the strong magnetic field (Staude, 1978; Knobloch and Weiss, 1984), or by forced oscillatory convection (Obridko, 1979). A first step towards a two-component modelling of the umbra has been made by Makita (1963), while Obridko (1974b, 1985; Obridko and Teplitskaya, 1978)) as well as Adjabshirzadeh and Koutchmy (1981) proposed detailed two-component models for the photospheric umbral layers. The earlier of these models assumed a hot secondary component the temperature of which is below that of the undisturbed photosphere, but in the latter model the secondary component is even hotter than the quiet photosphere.

Meanwhile new high-resolution sunspot observation at various wavelength regions have been published which suggest a revival of a two-component umbral model. Especially the suggestion of Obridko (1985) concerning a possible connection between the inhomogeneous structures at different heights should be worked out in more detail, even if such a suggestion is only a working hypothesis at present. In such a model the secondary component should consist of hot fine structures (bright points) in the photosphere, but cold, vertically elongated elements with TR temperatures at such heights were the main component already reaches coronal values. The filling factor for this secondary component would be about $\beta \approx 0.05$ to 0.10, without any significant variation with height. The exact value of β could differ, however, from spot to spot and also vary during the development of a single spot. Larger values of β seem to be related to 'active' phases of the development, e.g., the appearance of light bridges in the umbral photosphere seems to be correlated with the formation of bright plumes with strong emission in EUV lines formed at TR temperatures, but both phenomena are transient events in the spot's history. Recent observations by Kitai (1986) provide strong evidence for an extension of photospheric umbral dots to chromospheric levels; the chromospheric dots have smaller sizes, longer lifetimes, and smaller velocities than oscillations or flashes.

3. Outline of the two-component working model of the umbral atmosphere

3.1. *Photospheric and chromospheric layers*

Our development for the photospheric part of the umbral model started with the model of Obridko (1974b, 1985) which consists of two components in hydrostatic equilibrium, with temperature differences of $\Delta\theta = 0.48$ and 0.10 between the main and secondary components, respectively, and the mean undisturbed photosphere outside the spot ($\theta = 5040/T$).

For reference to the mean quiet atmosphere we used the VAL 3C model (Vernazza et al., 1981) which has been recalculated to test the accuracy of our own procedures; only the functions $T(m)$ and $v_{tu}(m)$ have been adapted from the original model. Here m is the column mass defined by $dm = -\rho\,dz$ with ρ = mass density, v_{tu} is the turbulent velocity which determines the turbulent pressure, $P_{tu} = \rho\, v_{tu}^2/2$, being related to the gas pressure P_G by the hydrostatic equilibrium relation (g is the surface gravity)

$$P_G + P_{tu} = gm. \tag{1}$$

Details of the computer routines have been described in previous papers (Staude, 1981, 1982). In agreement with these earlier calculations we assumed the chemical composition of the HSRA model (Gingerich et al., 1971) but added potassium as an electron donor at low temperatures. For a given set of local values of T and P_e (electron pressure) the ionization equilibria and the equation of state are solved by the method of Mihalas (1967) using a modified version of the STATE subroutine from the LINEAR code of Auer et al. (1972), while the opacities for a given wavelength λ are calculated by means of the CHIGEN subroutine from LINEAR.

In STATE the level population of the ground state of hydrogen is permitted to depart from LTE by a coefficient B1. In the present paper we used the analytic approximation for B1 quoted by Kneer and Mattig (1978, their Eq. (5) together with Appendix A1) which is valid for a two-level plus continuum hydrogen atom, with Ly α in detailed radiative balance, and for constant values of T, n_e, and the radiation temperature $T_{R,B}$ in the Balmer continuum for all heights above the point $T = T_{R,B}$ in the photo-

sphere. This simple non-LTE approach seems to be sufficient for our purposes because the much stronger effects on an inhomogeneous atmosphere will be considered here. For $T_{R,B}$, we used the following values: $T_{R,B} = 4940$ K for the VAL 3C model (in agreement with the data from Vernazza et al., 1981), $T_{R,B} = 4900$ K in the secondary component, and $T_{R,B} = 3500$ K in the main component of the umbra, the latter value being in agreement with Kneer and Mattig (1978) and Lites and Skumanich (1982). For the secondary component the assumed value of $T_{R,B}$ is probably an upper limit based on a neglect of lateral radiative transfer. Considering the small horizontal extent of the fine structures, dilution would cause an approach of $T_{R,B}$ to a value closer to that of the surroundings with increasing height in the chromosphere, because the Balmer continuum is optically thin here.

The influence of the assumptions in our procedures (B1, different chemical composition, etc.) can be illustrated by the differences between the original VAL 3C model and our recalculation: The geometrical height scale, or the extent between $z = 0$ and the top of the chromosphere, is increased by 7% in our model. The differences of P_G or ρ values at equal T are smaller than 5%, in most cases around 1%; for P_e the accuracy is better than 50% (this agrees with estimates of Kneer and Mattig, 1978), but better than 10% in the lower photosphere and upper chromosphere. B1 is more than two orders of magnitude too small in the upper chromosphere in our approximation, but this has little influence on the equation of state because hydrogen is almost completely ionized there; in the lower chromosphere the deviations are smaller than a factor of two.

For the umbral main component we started from the $T(m)$ run in the original homogeneous umbral model of Staude (1981) which has been recalculated with the simplified non-LTE procedure. The photospheric part of $T(\tau_0)$ of this model is close to that in Obridko's (1974b, 1985) main component; τ_0 is the optical depth in the continuum at $\lambda_0 = 500$ nm. The assumed run of $v_{tu}(m)$ differs somewhat from that in the original model: We used a monotonically increasing $v_{tu}(T)$ instead of the earlier complicated run (model S 15 instead of model S 05 in the notation of Žugžda et al., 1984). The differences to the original model are small; arguments in favour of this model will not be repeated here.

The secondary umbral component has a $T(\tau_0)$ dependence which is close to that in Obridko's secondary component in the photosphere. At higher levels we assumed a temperature minimum of $T_{min} \approx 3800$ K and a more extended lower chromosphere than that in the main component. Two variants of the secondary component have been tried: One has P_e values in the TR close to those in the main component (variant b), in the other model P_e is three times larger (variant a) which results in a smaller extent of the lower chromosphere. Details of the upper layers (TR) will be discussed in the next section.

Contrary to the results of Adjabshirzadeh and Koutchmy (1981) our secondary component is somewhat cooler than the quiet photosphere. The exact value of $\Delta\theta$ is difficult to determine due to the unresolved fine structure of umbral dots, the influence of stray light, and the uncertainty in tracing the continuum between the numerous lines especially in the violet spectral region. Obridko (1974b; Obridko and Teplitskaya, 1978) derived the value $\Delta\theta = 0.10$, together with a filling factor of $\beta = 0.05$ to 0.10, from the upper limit of brightness observations in umbrae and from empirical relations between brightness and magnetic field strengths. An indication of a lower intensity I in bright dots as

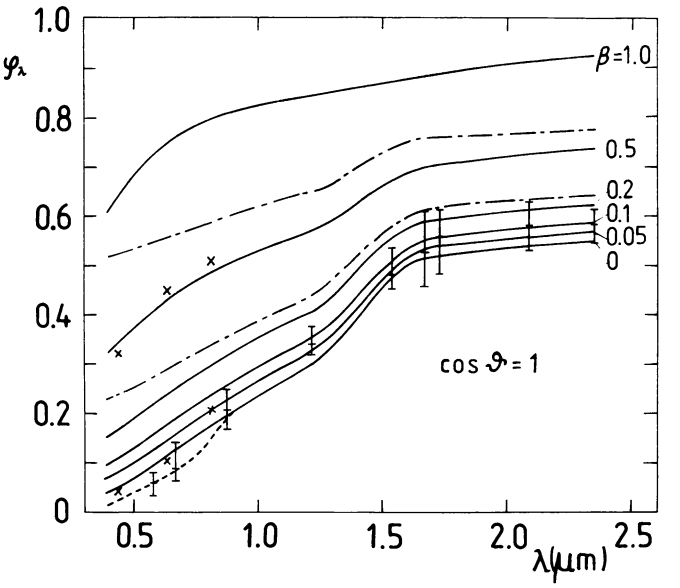

Fig. 1. Predicted continuum intensity contrast $\varphi = I$ (umbra)/I (quiet sun) versus wavelength λ for different filling factors of the two umbral components. $\beta = 0$: main component (cold in the photosphere). $\beta = 1$: only secondary component (bright dots). Dash-dot curves: modified variant using the quiet sun's photosphere for the secondary component. Crosses: high-resolution continuum observations by Wiehr and Stellmacher (1985), vertical bars: broad-band observations by Albregtsen and Maltby (1981). The dashed curve considers the lowering of the UV continuum by lines for $\beta = 0$

compared with the quiet photosphere has also been found by Abdussamatov (1980), and even light bridges seem to be cooler than the quiet sun (Firstova and Grigoryev, 1971). Hotter umbral dots are difficult to explain because their small horizontal dimensions of $\Delta\tau_0 \lesssim 1$ would result in fast radiative cooling. Grossmann-Doerth et al. (1986) found evidence that temperatures in dots are several 100 K up to more than 1000 K cooler than the quiet photosphere.

For comparison with continuum umbral observations we calculated the contrast $\varphi(\lambda) = I$(umbra)/I(quiet sun) for different filling factors β($\beta = 0$: only main component, $\beta = 1$: only secondary component). Figure 1 shows the results: Our two-component models with $\beta = 0.05$ to 0.10 fit the broad-band data from Albregtsen and Maltby (1981: vertical bars giving average values as well as upper and lower limits) if we additionally consider a lowering of the violet continuum by lines. The dashed curve indicates the latter effect for $\beta = 0$, here data for an opacity enhancement have been taken from Zwaan (1974) and Stellmacher and Wiehr (1981). The narrow-band, high-resolution continuum data of Wiehr and Stellmacher (1985: crosses in our Fig. 1) could be explained as well: The lowest intensities would correspond to $\beta \lesssim 0.05$, while the highest intensities are close to a model with $\beta = 0.50$. In agreement with Wiehr and Stellmacher (1985) we state that the observed $\varphi(\lambda)$ cannot be explained by umbral dots with $\Delta\theta \leq 0$. For instance, Fig. 1 includes two dash-dot curves for $\beta = 0.2$ and 0.5 where the secondary component agrees with the quiet photosphere: The gradient of $\varphi(\lambda)$ is too small here. The discrepancy would be still stronger for hotter dots.

Recently, Maltby et al. (1986) derived a detailed one-dimensional model atmosphere for the darkest parts of large umbrae. The $\varphi(\lambda)$ prediction from their model has been compared with

observations, similar to our test shown in Fig. 1, but also with the predictions from other models such as the WOSM. Because the WOSM is close to the main umbral component of the present paper, this comparison is interesting for our work. The values of $\varphi(\lambda)$ predicted from the WOSM seem to be somewhat too low in the infrared region, but this is not the case if we take into account a few percent of the secondary component, see Fig. 1. Maltby et al. (1966) also discussed the observed center-limb variation of $\varphi(\lambda)$ (Albregtsen et al., 1984) and compared it with the predictions from 3 models, that is from their own model, the WOSM, and a model of van Ballegooijen (1984). The WOSM seems to disagree with the observations around $\lambda = 1\,\mu$m, but it gives a better agreement than the other models in the infrared at $\lambda \gtrsim 1.5\,\mu$m. Of course, such a comparison will be influenced by the consideration of inhomogeneities, but for such an estimate a detailed knowledge of the geometrical shape of the inhomogeneities would be required which is not yet available.

Van Ballegooijen (1984) used observations which were averaged over a larger part of an umbra. From these data he found strong evidence for an inhomogeneous structure of the lower umbral photosphere: Different one-dimensional models were necessary to fit observed data in the umbral continuum and in various lines; $\Delta T = 460$ K is a lower limit for the required difference between hot and cold umbral elements at $\tau_0 = 3$. Our corresponding value of ΔT is almost five times larger, but it refers to the real temperatures in the two components of our model.

We assumed a value of $T_{\min} = 3000$ K for the main umbral component, in agreement with earlier results of Makita (1968) and Sotirovski (1971) from TiO lines, with the models of Stellmacher and Wiehr (1975) and Sobotka (1985a,b) based on profiles of strong lines, and with the interpretation of recent SiO band observations at 8 μm by Glenar et al. (1983). $T_{\min} \approx 3000$ K is also suggested from an interpretation of umbral oscillations by resonant transmission of magneto-atmospheric waves (Žugžda et al., 1983, 1987): The quality of such a resonator is quickly reduced if $T_{\min}$ is increased. Cooling in CO bands seems to produce values of $T_{\min} \lesssim 3000$ K in cool atmospheres (Muchmore and Ulmschneider, 1985). Recent suggestions of larger values of $T_{\min}$ (3350 K: Avrett and Kurucz, 1983; 3400 K: Maltby et al., 1986) assume one-dimensional umbral models which are surely influenced by the neglect of hot inhomogeneities. Sobotka (1985a,b) found $T_{\min} \lesssim 3000$ K for the umbrae of old, large, and stable spots, but larger values of $T_{\min} \gtrsim 3500$ K for small or fast developing sunspots.

The zero point of the geometrical height scale, $z = 0$, has been arbitrarily fixed at $\tau_0 = 0.1$ in the quiet sun. Then we assumed a Wilson depression of $\Delta z = 500$ km between the optical depths $\tau_0 = 0.1$ in the umbral main component and the quiet photosphere. Using the convective zone model of Spruit (1977) which has been fitted to an earlier version of the VAL model, we find that such a choice satisfies magnetohydrostatic equilibrium at $\tau_0 = 0.1$ in the umbra if a vertical magnetic field of $B = 3500$ G is assumed: also the values of ρ inside and outside the umbra are then in agreement. The magnetic field strength could be smaller ($2\,\text{kG} \leq B \leq 3.5\,\text{kG}$ in our case according to Maltby, 1977) if the tension of the lines of force of the magnetic field diverging with height is taken into account. For the secondary component we assumed a depression of $\Delta z = 200$ km of its $\tau_0 = 0.1$ level relative to that in the quiet sun. Hydrostatic equilibrium between such a fine structure element and the surrounding main component is achieved if the field strength in the dot is only slightly

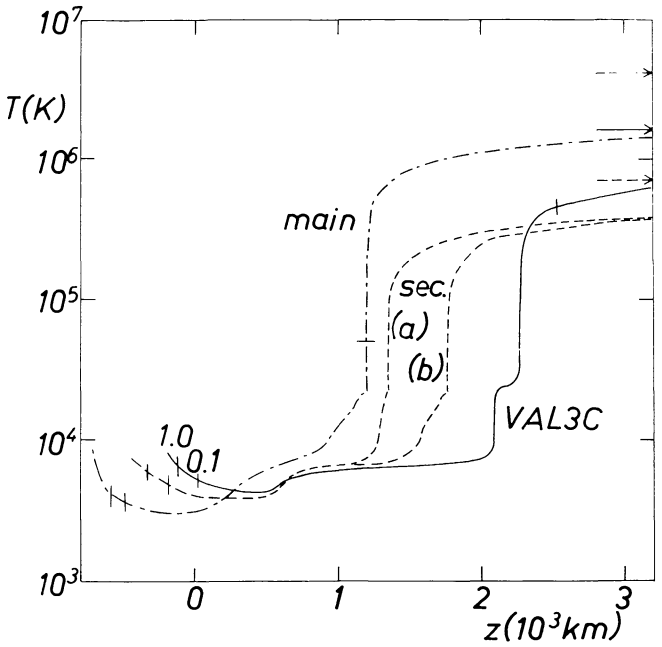

Fig. 2. Temperature T versus geometrical height z for the proposed models. The arrows on the right-hand side indicate the values T_c which are asymptotically approached for $z \to \infty$. Small bars mark the positions of $\tau_0 = 1.0$, $\tau_0 = 0.1$, and of the starting points of the TR model on the different curves

(a few percent at equal τ) smaller than that in the main component. This is in agreement with many high-resolution observations which resulted in values of B in bright dots which hardly differed from those in the dark umbral main component (Zwaan et al., 1985; Adjabshirzadeh and Koutchmy, 1983; Abdussamatov, 1975).

The resulting models are listed in Table 1a–1c; Fig. 2 shows the corresponding $T(z)$ curves, Fig. 3 the $P_e(z)$ relation, and Fig. 4 gives the wavelength dependence of the geometrical heights z where the optical depths $\tau(\lambda) = 0.1$ and 1.0 for each component.

Figure 5 illustrates the magnetohydrostatic equilibrium between both umbral components at photospheric levels. For simplicity a pure vertical magnetic field of $B_{\text{main}} = 3$ kG has been assumed for the main component, while $B_{\text{sec}}(z)$ has been calculated assuming an axially symmetrical thin flux tube for a fine structure element of the secondary component. B_{sec} decreases with increasing depth, but magnetic fields will be measured at nearly equal optical depths, and there we find indeed the conditions mentioned above: at $\tau_0 = 0.1$ in both models the field strengths show a difference of only 6 percent in our case. Figure 5 also shows that the filling factor β remains almost constant over a large range of heights.

However, an apparent centre-limb variation of β (an increase in most cases) could be observed due to projection effects which will depend on the aspect ratio, that is on the ratio of the heights (about 300 km) to the horizontal diameters of the flux tubes for a given τ.

3.2. *Transition region and lower corona*

The structure of the TR and corona in our two-component umbral model closely follows that of the WOSM (Staude et al., 1983, 1984) as outlined in Sect. 2. A few differences should be

Table 1a. Umbral main component, photosphere and chromosphere, cgs units. $m_0 = 1.8 - 5$ ($= 1.8\,10^{-5}$), $z_a = -5.0 + 7$.

$m - m_0$	$z - z_a$	$\tau_0(\lambda_0 = 500\,\text{nm})$	T	P_e	P_G	ρ
6.99 − 7	1.7033 + 8	1.579 − 10	4.600 + 4	2.273 − 1	4.546 − 1	7.696 − 14
7.00	1.7031	5.310	4.200	2.260	4.520	8.381
7.02	1.7029	1.143 − 9	3.900	2.272	4.545	9.075
7.05	1.7026	1.984	3.600	2.266	4.532	9.803
7.10	1.7021	3.626	3.200	2.255	4.510	1.098 − 13
7.12 − 7	1.7019 + 8	4.316 − 9	3.000 + 4	2.243 − 1	4.485 − 1	1.164 − 13
7.15	1.7017	5.133	2.800	2.229	4.457	1.240
7.18	1.7014	6.102	2.600	2.213	4.426	1.326
7.21	1.7012	7.105	2.400	2.200	4.401	1.428
7.25	1.7010	8.270	2.200	2.212	4.424	1.566
1.364 − 6	1.662 + 8	2.061 − 7	2.100 + 4	2.279 − 1	4.559 − 1	1.691 − 13
1.587	1.649	2.752	2.000	2.296	4.593	1.789
1.805	1.637	3.427	1.900	2.315	4.632	1.899
2.077	1.623	4.269	1.800	2.338	4.680	2.026
2.442	1.606	5.399	1.700	2.371	4.748	2.178
2.904 − 6	1.585 + 8	6.826 − 7	1.600 + 4	2.412 − 1	4.835 − 1	2.358 − 13
3.494	1.561	8.643	1.500	2.467	4.956	2.584
4.241	1.534	1.093 − 6	1.400	2.531	5.107	2.866
5.028	1.508	1.330	1.300	2.568	5.245	3.206
5.989	1.480	1.608	1.200	2.549	5.392	3.690
6.957 − 6	1.456 + 8	1.854 − 6	1.100 + 4	2.341 − 1	5.509 − 1	4.485 − 13
8.102	1.434	2.074	1.000	1.892	5.699	5.930
1.086 − 5	1.395	2.386	9.000 + 3	1.185	6.392	9.011
1.889	1.322	2.765	8.000	5.504 − 2	7.934	1.437 − 12
5.247	1.156	3.247	7.000	2.482	1.542 + 0	3.375
6.700 − 5	1.118 + 8	3.308 − 6	6.700 + 3	1.894 − 2	1.982 + 0	4.563 − 12
1.160 − 4	1.034	3.421	6.250	1.275	3.258	8.088
2.436	9.198 + 7	3.542	5.700	7.774 − 3	6.519	1.779 − 11
4.463	8.355	3.618	5.000	3.851	1.190 + 1	3.707
6.841	7.848	3.663	4.500	2.275	1.852	6.408
1.061 − 3	7.386 + 7	3.742 − 6	4.000 + 3	2.540 − 3	2.862 + 1	1.114 − 10
2.477	6.510	4.297	3.500	3.024	6.624	2.948
4.344	6.026	5.260	3.250	2.170	1.162 + 2	5.571
1.103 − 2	5.202	9.145	3.100	2.270	2.952	1.491 − 9
3.513	4.153	3.103 − 5	3.000	3.642	9.380	5.009
2.101 − 1	2.126 + 7	4.806 − 4	3.063 + 3	1.629 − 2	5.600 + 3	3.126 − 8
2.942	1.896	8.609	3.091	2.251	7.842	4.392
4.113	1.667	1.543 − 3	3.134	3.204	1.097 + 4	6.100
5.840	1.424	2.874	3.193	4.766	1.558	8.521
8.723	1.140	5.922	3.258	7.452	2.328	1.254 − 7
1.353 + 0	8.213 + 6	1.320 − 2	3.341 + 3	1.244 − 1	3.612 + 4	1.900 − 7
2.116	4.894	3.014	3.427	2.094	5.652	2.906
3.298	1.518	6.910	3.523	3.583	8.817	4.410
5.128	−1.937 + 6	1.602 − 1	3.635	6.314	1.372 + 5	6.628
7.945	−5.495	3.788	3.769	1.160 + 0	2.128	9.829
1.223 + 1	−9.194 + 6	9.356 − 1	3.964 + 3	2.416 + 0	3.280 + 5	1.410 − 6
1.834	−1.301 + 7	2.552 + 0	4.350	7.287	4.932	1.847
2.605	−1.699	7.664	5.400	4.301 + 1	7.036	2.041
3.398	−2.081	2.486 + 1	6.810	3.465 + 2	9.204	2.106
3.744	−2.257	6.554	8.520	4.345 + 3	1.017 + 6	1.851

Table 1b. Umbral secondary component, 'thick' variant (a), photosphere and chromosphere, cgs units. $m_0 = 5.7 - 5$, $z_b = -2.0 + 7$.

$m - m_0$	$z - z_b$	$\tau_0(\lambda_0 = 500\,\text{nm})$	T	P_e	P_G	ρ
1.006 − 6	1.5427 + 8	1.000 − 11	4.600 + 4	6.859 − 1	1.372 + 0	2.322 − 13
1.010	1.5425	1.248 − 9	4.200	6.822	1.364	2.530
1.014	1.5424	2.487	3.600	6.878	1.376	2.576
1.019	1.5422	4.036	3.200	6.841	1.368	3.330
1.025	1.5420	5.896	2.600	6.723	1.345	4.028
1.032 − 6	1.5419 + 8	8.068 − 9	2.200 + 4	6.618 − 1	1.324 + 0	4.686 − 13
1.515	1.5319	1.580 − 7	2.100	6.729	1.346	4.992
1.688	1.5285	2.118	2.000	6.721	1.344	5.236
2.067	1.5216	3.295	1.800	6.698	1.340	5.800
2.717	1.5110	5.315	1.600	6.710	1.344	6.548
3.713 − 6	1.497 + 8	8.403 − 7	1.400 + 4	6.720 − 1	1.350 + 0	7.548 − 13
4.861	1.483	1.185 − 6	1.200	6.513	1.354	9.115
5.635	1.475	1.384	1.000	5.424	1.308	1.192 − 12
1.098 − 5	1.440	2.230	8.000 + 3	3.047	1.341	2.017
3.941	1.336	3.811	6.700	1.001	1.960	4.324
4.904 − 5	1.316 + 8	3.967 − 6	6.600 + 3	9.183 − 2	2.165 + 0	4.892 − 12
9.503	1.237	4.560	6.500	9.629	3.121	7.247
1.643 − 4	1.157	5.228	6.400	1.010 − 1	4.567	1.087 − 11
2.387	1.098	5.797	6.350	1.090	6.150	1.482
3.101	1.055	6.266	6.300	1.131	7.689	1.873
3.890 − 4	1.017 + 8	6.708 − 6	6.200 + 3	1.073 − 1	9.480 + 0	2.355 − 11
4.893	9.786 + 7	7.174	6.100	1.017	1.178 + 1	2.983
6.055	9.436	7.627	6.000	9.549 − 2	1.450	3.740
7.608	9.068	8.111	5.800	7.501	1.811	4.843
1.032 − 3	8.591	8.706	5.500	4.912	2.431	6.871
1.303 − 3	8.247 + 7	9.094 − 6	5.200 + 3	2.958 − 2	3.090 + 1	9.247 − 11
1.603	7.966	9.346	4.700	1.052	3.816	1.264 − 10
2.540	7.400	9.837	4.150	6.181 − 3	6.366	2.389
6.379	6.307	1.306 − 5	3.820	1.048 − 2	1.630 + 2	6.647
2.893 − 2	4.248	6.730	3.810	3.372	7.592	3.105 − 9
8.638 − 2	3.016 + 7	3.966 − 4	3.829 + 3	7.614 − 2	2.301 + 3	9.371 − 9
1.075 − 1	2.813	5.766	3.841	9.088	2.878	1.169 − 8
1.312	2.629	8.113	3.862	1.091 − 1	3.524	1.424
1.504	2.502	1.029 − 3	3.877	1.235	4.042	1.627
2.024	2.222	1.729	3.919	1.651	5.438	2.166
2.792 − 1	1.914 + 7	3.067 − 3	3.981 + 3	2.339 − 1	7.505 + 3	2.944 − 8
3.682	1.647	5.077	4.051	3.254	9.900	3.816
4.323	1.490	6.837	4.104	4.026	1.162 + 4	4.423
5.986	1.162	1.268 − 2	4.232	6.362	1.610	5.941
8.375	8.122 + 6	2.432	4.394	1.045 + 0	2.255	8.008
1.116 + 0	5.036 + 6	4.255 − 2	4.553 + 3	1.599 + 0	3.005 + 4	1.030 − 7
1.323	3.160	5.930	4.675	2.098	3.565	1.189
1.886	−9.638 + 5	1.173 − 1	4.946	3.602	5.087	1.604
2.743	−5.594 + 6	2.390	5.272	6.504	7.407	2.190
3.250	−7.793	3.369	5.612	1.104 + 1	8.785	2.439
4.637 + 0	−1.272 + 7	7.337 − 1	5.860 + 3	2.075 + 1	1.254 + 5	3.334 − 7
6.179	−1.691	1.596 + 0	6.364	6.116	1.672	4.093
7.794	−2.055	3.389	6.765	1.440 + 2	2.111	4.859
9.363	−2.357	6.430	7.109	2.863	2.538	5.554
1.032 + 1	−2.523	9.123	7.315	4.208	2.797	5.947

Table 1c. Umbral secondary component, 'thin' variant (b), photosphere and chromosphere, cgs units. $m_0 = 1.77 - 5$, $z_b = -2.0 + 7$.

$m - m_0$	$z - z_0$	$\tau_0(\lambda_0 = 500\,\mathrm{nm})$	T	P_e	P_G	ρ
1.002 − 6	2.0297 + 8	1.000 − 11	4.600 + 4	2.562 − 1	5.124 − 1	8.675 − 14
1.006	2.0293	1.248 − 9	4.200	2.225	4.450	8.250
1.010	2.0288	2.486	3.600	2.193	4.385	9.486
1.015	2.0283	4.033	3.200	2.224	4.449	1.083 − 13
1.021	2.0278	5.891	2.600	2.183	4.367	1.308
1.028 − 6	2.027 + 8	8.058 − 9	2.200 + 4	2.153 − 1	4.307 − 1	1.525 − 13
1.511	1.997	1.576 − 7	2.100	2.213	4.426	1.642
1.684	1.987	2.112	2.000	2.251	4.503	1.754
2.063	1.966	3.286	1.800	2.265	4.530	1.960
2.713	1.935	3.299	1.600	2.308	4.620	2.250
3.709 − 6	1.894 + 8	8.378 − 7	1.400 + 4	2.386 − 1	4.785 − 1	2.669 − 13
4.857	1.855	1.186 − 6	1.200	2.419	4.942	3.274
5.631	1.834	1.394	1.000	2.137	4.907	4.314
1.098 − 5	1.737	2.380	8.000 + 3	1.587	5.450	7.522
3.940	1.484	4.545	6.700	7.060 − 2	1.022 + 0	2.213 − 12
4.903 − 5	1.446 + 8	4.746 − 6	6.600 + 3	7.199 − 2	1.366 + 0	3.055 − 12
9.502	1.328	5.447	6.500	8.231	2.310	5.338
1.643 − 4	1.224	6.185	6.400	9.107	3.740	8.878
2.387	1.153	6.788	6.350	1.010 − 1	5.302	1.276 − 11
3.101	1.104	7.275	6.300	1.064	6.822	1.660
3.890 − 4	1.061 + 8	7.729 − 6	6.200 + 3	1.015 − 1	8.506 + 0	2.111 − 11
4.893	1.019	8.203	6.100	9.706 − 2	1.076 + 1	2.721
6.055	9.807 + 7	8.661	6.000	9.173	1.342	3.459
7.608	9.411	9.146	5.800	7.247	1.695	4.531
1.032 − 3	8.903	9.738	5.500	4.774	2.302	6.506
1.303 − 3	8.540 + 7	1.012 − 5	5.200 + 3	2.869 − 2	2.920 + 1	8.736 − 11
1.603	8.243	1.037	4.700	1.019	3.621	1.200 − 10
2.540	7.636	1.084	4.150	5.656 − 3	5.759	2.161
6.379	6.445	1.391	3.820	1.008 − 2	1.554 + 2	6.338
2.893 − 2	4.290	6.668	3.810	3.287	7.332	2.998 − 9
8.638 − 2	3.020 + 7	3.911 − 4	3.829 + 3	7.530 − 2	2.264 + 3	9.219 − 9
1.075 − 1	2.814	5.698	3.841	9.058	2.863	1.163 − 8
1.312	2.630	8.039	3.862	1.087 − 1	3.508	1.418
1.504	2.502	1.021 − 3	3.877	1.235	4.041	1.626
2.024	2.223	1.721	3.919	1.651	5.437	2.166
2.792 − 1	1.915 + 7	3.059 − 3	3.981 + 3	2.338 − 1	7.504 + 3	2.943 − 8
3.682	1.647	5.069	4.051	3.253	9.900	3.816
4.323	1.490	6.828	4.104	4.026	1.162 + 4	4.423
5.986	1.163	1.267 − 2	4.232	6.362	1.610	5.540
8.375	8.123 + 6	2.431	4.394	1.045 + 0	2.255	8.008

Deeper layers coincide with the 'thick' variant (a), Table 1b

mentioned here: In the WOSM simple analytic expression for $T(z)$ and $P_e(z)$ have been used for each component assuming complete ionization (valid for $T \gtrsim 5\,10^4$ K), hydrostatic equilibrium, and a constant conductive heat flux F_c. The latter condition $F_c = \text{const}$ seems unreal at higher coronal levels and has now been replaced by another condition (Staude, 1985): Following Jordan (1980) we use a power law for the emission measure,

$$EM = \int_{\Delta} n_e^2 (dT/dz)^{-1}\, dT = aT^b, \tag{2}$$

with constant values of a and b. In agreement with Jordan (1980) we assume for Δ, the line-forming range, a value of $\Delta \log T = 0.3$, and a power of $b = 1.5$. With $d = (b + 1)$ we obtain in cgs units

$$a = 1.74\,10^3\, dP_0^2 (T_c^d - T_0^d)^{-1}, \tag{3}$$

$$dT/dz = 4.05\,10^{-4}((T/T_c)^{-d} - 1)/d, \tag{4}$$

$$P^2 = P_0^2 (T_c^d - T^d)/(T_c^d - T_0^d). \tag{5}$$

T_c is the coronal value of T which is asymptotically approached if $z \to \infty$ or $P \to 0$. P_0 is the value of P_e at the base of the TR

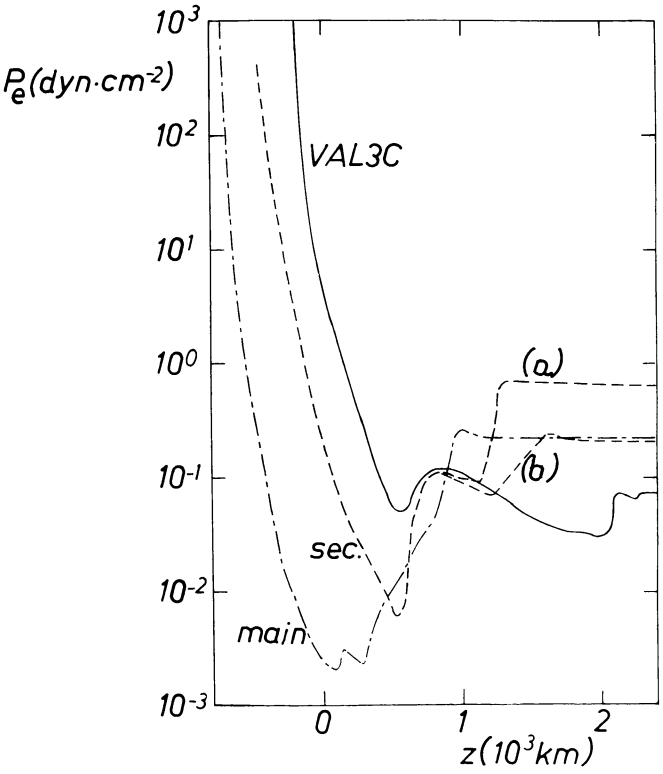

Fig. 3. Electron pressure P_e versus z for the proposed models

which is taken at $T_0 = 5\,10^4$ K. The subscript e has been omitted from P because Eq. (5) is also valid for $P_G \approx 2P_e$. In a recent paper by Staude (1985) the results from Eqs. (2–5) have been compared with the earlier analytic expressions for $F_c = \text{const}$ and with observations which confirmed the basic features of the WOSM. The $T(z)$ relation (4) is completely determined by the coronal value T_c which replaces the parameter F_c in the earlier version. Both types of models nearly coincide in the lower TR at $T^d \ll T_c^d$ were they are related to each other by

$$F_c \approx 1.78\,10^{-10}\,T_c^{5/2} \qquad (6)$$

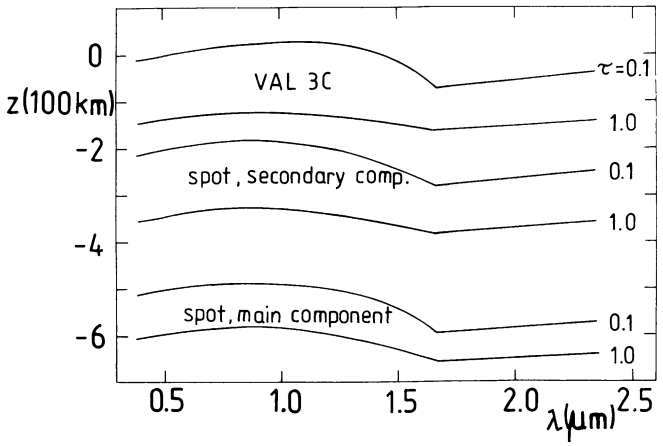

Fig. 4. Wavelength dependence of the geometrical heights z where the optical depths $\tau(\lambda) = 0.1$ (mean depth of formation of medium-strong lines) and $\tau(\lambda) = 1.0$ (continuum at disk center, $\mu = 1$) are situated

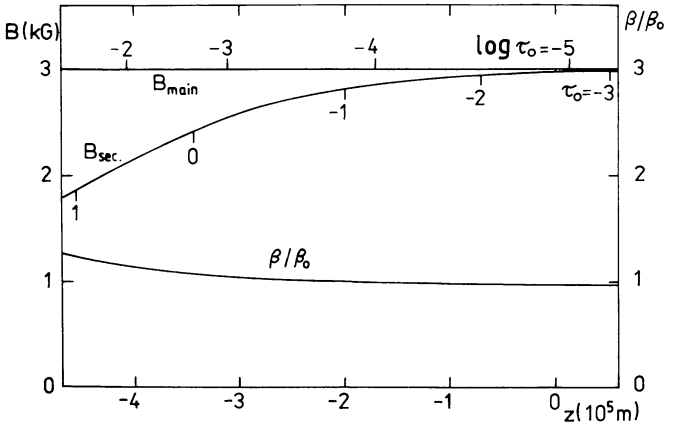

Fig. 5. Height dependence of the magnetic field strength B in the umbral main component (B assumed constant) and in the secondary component (thin flux tube) as well as of the filling factor β (normalized to the value β_0 at $\tau_0(\text{sec}) = 0.1$). The optical depths log τ_0 for the 2 components are marked in the $B(z)$ curves

if $b = 1.5$, but in this case also $P = \text{const}$ is a good approximation for Eq. (5).

Our chromospheric models as described in Sect. 3.1 are now extrapolated towards TR and corona using Eqs. (4, 5) with the parameters $T_c = 1.6\,10^6$ K for the VAL 3C, $7\,10^5$ K for the two variants of the secondary component, and $4\,10^6$ K for the umbral main component; the results are listed in Table 2 and included in Figs. 2 and 3. The differences between main and secondary umbral components in the corona are somewhat smaller than in the WOSM which gives a better agreement with recent EUV data (Staude, 1985). The value $T_c = 4\,10^6$ K for the main component seems rather large, but we have values of $T = 10^6$ K at $\Delta z = 2.26$ Mm above the umbral photosphere ($\tau_0 = 1$) and $T = 2\,10^6$ K at $\Delta z = 8.68$ Mm.

Larger heights cannot be considered as parts of the umbral atmosphere: The diverging magnetic lines of force will turn out of the column above the photospheric umbra and joint with the loops above the penumbra and active region surrounding the sunspot where higher temperatures are often observed in microwave and X-ray data.

In a recent paper (Staude, 1985) it has been shown that the parameters T_c mentioned above, together with a value of P_0 which is three times larger in the secondary component (model (a)) as compared with the main component, can explain the EUV data of Nicolas et al. (1982); the necessary filling factor is $\beta = 0.07$. The value of P_0 in the secondary component seems to be smaller and closer to that in the main component if we consider sunspots in a 'quiescent' phase of its development (Kingston et al., 1982), that is in a phase without strong EUV plumes and associated mass motions. For such cases we derived our variant (b) of the secondary component.

A comprehensive investigation of the EUV spectrum from a sunspot with plumes has recently been published by Noyes et al. (1985) and Doyle et al. (1985) who found reasonable agreement between their measured line intensities and intensities calculated from our WOSM. This agreement is limited, however, to lines formed below $T = 2\,10^5$ K, while the measured intensities from lines formed above $4\,10^5$ K are an order of magnitude stronger than the predicted values. The WOSM has not been fitted to

Table 2a. Umbral main component, transition region and corona, cgs units, $z_a = -5.0 + 7 (= -5.0\,10^7)$

$z - z_a$	T	P_e
1.7034 + 8	5.00 + 4	2.284 − 1
1.7034	6.00	2.283
1.7034	7.00	2.283
1.7035	8.00	2.283
1.7035	9.00	2.283
1.7036 + 8	1.00 + 5	2.283 − 1
1.7037	1.20	2.283
1.7041	1.50	2.283
1.7054	2.00	2.283
1.7077	2.50	2.282
1.712 + 8	3.00 + 5	2.282 − 1
1.717	3.50	2.281
1.726	4.00	2.280
1.737	4.50	2.279
1.752	5.00	2.277
1.796 + 8	6.00 + 5	2.274 − 1
1.863	7.00	2.269
1.959	8.00	2.263
2.090	9.00	2.256
2.265	1.00 + 6	2.248
2.779 + 8	1.20 + 6	2.227 − 1
4.106	1.50	2.183
8.682	2.00	2.072
1.850 + 9	2.50	1.898
3.896	3.00	1.635
8.701 + 9	3.50 + 6	1.217 − 1
1.291 + 10	3.70	9.609 − 2
2.293	3.90	5.655
2.957	3.95	4.018

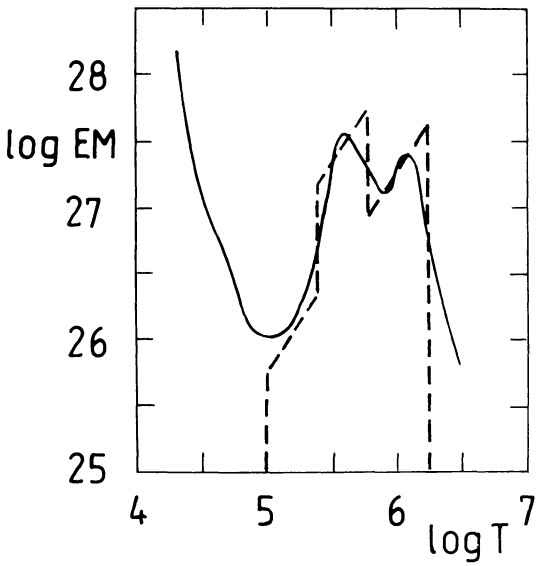

Fig. 6. Sunspot emission measure EM versus T. Observations by Noyes et al. (1985) and Doyle et al. (1985) – full curve- and prediction for a simple two-component model for $T > 10^5$ K – dashed curve

Table 2b. Umbral secondary component, transition region and corona, cgs units, $z_b = -2.0 + 7$

'Thick' variant (a)			'Thin' variant (b)	
$z - z_b$	P_e	T	$z - z_b$	P_e
1.5430 + 8	6.858 − 1	5.00 + 4	1.9653 + 8	2.237 − 1
1.5435	6.856	5.50	1.9657	2.237
1.5441	6.855	6.00	1.9663	2.236
1.5448	6.853	6.50	1.9671	2.236
1.5457	6.852	7.00	1.9680	2.235
1.548 + 8	6.847 − 1	8.00 + 4	1.970 + 8	2.234 − 1
1.551	6.842	9.00	1.974	2.232
1.556	6.836	1.00 + 5	1.978	2.230
1.568	6.821	1.20	1.990	2.225
1.599	6.789	1.50	2.021	2.215
1.700 + 8	6.711 − 1	2.00 + 5	2.122 + 8	2.189 − 1
1.894	6.596	2.50	2.316	2.152
2.227	6.437	3.00	2.650	2.100
2.763	6.226	3.50	3.185	2.031
3.590	5.956	4.00	4.012	1.943
4.843 + 8	5.611 − 1	4.50 + 5	5.226 + 8	1.831 − 1
6.747	5.176	5.00	7.169	1.688
9.716	4.618	5.50	1.014 + 9	1.506
1.467 + 9	3.881	6.00	1.510	1.266
2.457	2.822	6.50	2.500	9.206 − 2
3.256 + 9	2.210 − 1	6.70 + 5	3.298 + 9	7.210 − 2
5.072	1.290	6.90	5.116	4.208
6.250	9.146 − 2	6.95	6.294	2.984
7.829	5.800	6.98	7.873	1.890

data from a sunspot with a strong plume but considered a 'thin' secondary component, similar to our present variant (b), therefore the disagreement for $T \geq 4\,10^5$ K is not surprising. Now we tried to explain the emission measure (EM) data of Doyle et al. (1985) by a two-component model similar to our present model: Fig 6 shows that for $T \geq 10^5$ K the EM(T) curve of Doyle et al. can be roughly fitted by a model with $T_c = 1.8\,10^6$ K and $6\,10^5$ K for the main and secondary components, respectively, assuming additionally a value of P_0 which is three times larger in the secondary component. A volume filling factor of $\beta = 0.04$ for the plume (secondary component) is then sufficient, but this matter should only exist at temperatures above $T_0 = 2.5\,10^5$ K. Of course, the assumption of hydrostatic equilibrium seems questionable for such downflowing gas. However, other assumptions for the plume, such as falling gas which is radiatively cooling at constant pressure, would lead to similar results and not conflict with the data of Doyle et al. (1985).

4. Conclusions

Inhomogeneous structures are evident at all height levels in the atmosphere of a sunspot umbra. There are clear indications of a secondary, fine structure component consisting of thin threads which are extended in vertical direction along the magnetic field. In the present paper we tried to derive consequently a two-com-

ponent umbral model for all heights from the deepest photospheric layers up to the lower corona. The model is based on uniform physical assumptions for both umbral components and the quiet atmosphere for reference, including a common geometrical height scale. Such semi-empirical working models are justified by their capacity of expaining as many observations as possible and avoiding some contradictions of earlier models. This could indeed be achieved: The photospheric part of the models is able to predict, e.g., umbral continuum contrasts in agreement with recent measurements within the observational errors, and high-resolution measurements of magnetic field strengths are explained as well. The predicted emission from chromospheric and coronal levels, including the transition region between both, is in agreement with X-ray, EUV, and microwave observations of sunspots (Staude, 1981, 1985; Staude et al., 1983). Oscillations of velocity and intensity as observed in chromospheric and TR lines can be interpreted by a chromospheric resonator for slow-mode magneto-atmospheric waves in an atmosphere similar to our present model (Žugžda et al., 1983, 1984, 1987; Staude et al., 1985). The model should be tested and improved if new and better observed data become available, in the same way as our present model implies an attempt to improve our earlier Wroclaw-Ondrejov sunspot model. Further tests of the two-component model are being prepared and will include line profiles and umbral oscillations. Especially the basic hypothesis of a direct physical connection between the fine structures in the umbral photosphere and the transition region via the chromosphere should be verified by additional observed data and model calculations.

Several simplifying assumptions in our approach need a more detailed investigation in the future. The simple approximation for deviations from LTE should be replaced by more detailed calculations. The assumption of hydrostatic equilibrium seems doubtful at least for a plume with strong downflows, although the results do not differ very much from a calculation for constant pressure (as assumed, e.g., for a downstreaming and cooling gas). The two components of the model are supposed to represent vertical columns of plasma in the umbra which are completely independent from each other; future work should take into account the influence of horizontal radiative transfer which could influence the temperature distribution (Obridko, 1985, summarized some earlier papers in Chapter 9 of his book) as well as the formation of spectral lines (Stenholm and Stenflo, 1978).

We derived an average two-component model for a 'typical' large sunspot umbra. Future work should consider the dependence of the atmospheric structure on the phase of the solar cycle (Albregtsen et al., 1984; Maltby et al., 1986) and the phase of the evolution of a single spot. Sobotka (1985) found clear differences in the umbral photosphere of small sunspots depending on their diameter, but much smaller differences for large spots.

It would be highly desirable to get more complete observed data, that means observations of a single sunspot with high spectral and spatial resolutions which should be obtained simultaneously at many different wavelengths from X-rays to microwaves, but also in different phases of the development of a spot and with high time resolution to record the umbral oscillations at different height levels. Such data could help to correct the uncertain features of our present working model. In this way we could place at disposal improved information on plasma parameters which is necessary for further investigations of physical processes in a magnetized atmosphere such as the sunspot umbra.

References

Abdussamatov, H.I.: 1975, *Soln. dannye* **4**, 83
Abdussamatov, H.I.: 1980. *Soln. dannye* **11**, 99
Adjabshirzadeh, A., Koutchmy, S.: 1983, *Astron. Astrophys.* **122**, 1
Albregtsen, F., Maltby, P.: 1981, in *The Physics of Sunspots*, Proc. Sacramento Peak Observ. Conferences, p. 127
Albregtsen, F., Joràs, P.B., Maltby, P.: 1984, *Solar Phys.* **90**, 17
Auer, L.H., Heasley, J.N., Milkey, R.W.: 1972, *Kitt Peak National Observ. Contrib.* No. **555**
Avrett, E.H.: 1981, in *The Physics of Sunspots*, Proc. Sacramento Peak Observ. Conference, p. 235
Bumba, V., Hejna, L., Suda, J.: 1975, *Bull. Astron. Inst. Czechosl.* **26**, 315
Doyle, J.G., Raymond, J.C., Noyes, R.W., Kingston, A.E.: 1985, *Astrophys. J.* **297**, 816
Firstova, N.M., Grigoryev, V.M.: 1971, *Issled. po Geomagn., Aeron. i Fizike Solntsa* **20**, 185
Gingerich, O., Noyes, R.W., Kalkofen, W., Cuny, Y.: 1971, *Solar Phys.* **18**, 347
Glenar, D.A., Deming, D., Jennings, D.E., Kostiuk, I., Mumma, M.J.: 1983, *Astrophys. J.* **269**, 309
Grossmann-Doerth, U., Schmidt, W., Schröter, E.H.: 1986, *Astron. Astrophys.* **156**, 347
Gurman, J.B.: 1984, *Solar Phys.* **90**, 13
Jordan, G.: 1980, *Astron Astrophys.* **86**, 355
Kingston, A.E., Doyle, J.G., Dufton, P.L., Gurman, J.B.: 1982, *Solar Phys.* **81**, 47
Kitai, R.: 1986, *Solar Phys.* **104**, 287
Kneer, F., Mattig, W.: 1978, *Astron. Astrophys.* **65**, 17
Knobloch, E., Weiss, N.O.: 1984, *Monthly Notices Roy. Astron. Soc.* **207**, 203
Lites, B.W., Skumanich, A.: 1981, in *The Physics of Sunspots*, Proc Sacrament Peak Observ. Conference, p. 152
Lites, B.W., Skumanich, A.: 1982, *Astrophys. J. Suppl.* **49**, 293
Loughhead, R.E., Bray, R.J., Tappere, E.J.: 1979, *Astron. Astrophys.* **79**, 128
Makita, M.: 1963, *Publ. Astron. Soc. Japan* **15**, 145
Makita, M.: 1968, *Solar Phys.* **3**, 557
Maltby, P.: 1977, *Solar Phys.* **55**, 335
Maltby, P., Avrett, E.H., Carlsson, M., Kjeldseth-Moe, O., Kurucz, R.L., Loeser, R.: 1986; *Astrophys. J.* **306**, 284
Mihalas, D.: 1967, *Methods Comp. Phys.* **7**, 1
Muchmore, D., Ulmschneider, P.: 1985, *Astron. Astrophys.* **142**, 393
Nicolas, K.R., Kjeldseth Moe, O., Bartoe, J.-D.F., Brueckner, G.E.: 1982, *Solar Phys.* **81**, 253
Noyes, R.W., Raymond, J.C., Doyle, J.G., Kingston, A.E.: 1985, *Astrophys. J.* **297**, 805
Obridko, V.N.: 1974a, *Astron. Zh.* **51**, 1272
Obridko, V.N.: 1974b, *Soln. dannye* **4**, 72
Obridko, V.N.: 1979, *Soln. dannye* **3**, 72
Obridko, V.N.: 1985, *Sunspots and Complexes of Activity* (in Russian), Nauka, Moskva
Obridko, V.N., Teplitskaya, R.B.: 1978, *Astronomiya.* **14**, 7
Parker, E.N.: 1979, *Astrophys. J.* **234**, 333
Sobotka, M.: 1985a, *Bull. Astron. Inst. Czechosl.* **36**, 230
Sobotka, M.: 1985b, *Astron. Zh.* **62**, 995
Sotirovski, P.: 1971, *Astron. Astrophys.* **14**, 319
Spruit, H.C.: 1977, Thesis Utrecht

Staude, J.: 1978, *Bull. Astron. Inst. Czechosl.* **29**, 71
Staude, J.: 1981, *Astron. Astrophys.* **100**, 284
Staude, J.: 1982, HHI-STP-Report No. **14**, Zentralinstitut für solar-terrestrische Physik, Berlin, 24
Staude, J.: 1985, *Astron. Nachr.* **306**, 197
Staude, J., Fürstenberg, F., Hildebrandt, J., Krüger, A., Jakimiec, J., Obridko, V.N., Siarkowski, M., Sylwester, B., Sylwester, J.: 1983, *Acta Astron.* **33**, 441;
Staude, J., et al.: 1984, *Astron. Zh.* **61**, 956
Staude, J., Žugžda, Y.D., Locāns, V.: 1985, *Solar Phys.* **95**, 37
Stellmacher, G., Wiehr, E.: 1975, *Astron. Astrophys.* **45**, 69
Stellmacher, G., Wiehr, E.: 1981, *Astron. Astrophys.* **95**, 229
Stenholm, L.G., Stenflo, J.O.: 1978, *Astron. Astrophys.* **67**, 33
Teplitskaya, R.B., Grigoryeva (Effendieva), S.A., Skochilov, V.G.: 1978, *Solar Phys.* **56**, 293
van Ballegooijen, A.A.: 1984, *Solar Phys.* **91**, 195
Vernazza, J.E., Avrett, E.H., Loeser, R.: 1981, *Astrophys. J. Suppl.* **45**, 635
Wiehr, E., Stellmacher, G.: 1985, High Resolution in Solar Physics, *Lect. Notes Phys.* **233**, 254
Žugžda, Y.D., Locāns, V., Staude, J.: 1983, *Solar Phys.* **82**, 369
Žugžda, Y.D., Locāns, V., Staude, J.: 1987, *Astron. Nachr.* **308**, 257
Žugžda, Y.D., Staude, J., Locāns, V.: 1984, *Solar Phys.* **91**, 219
Zwaan, C.: 1974, *Solar Phys.* **37**, 99
Zwaan, C., Brants, J.J., Cram, L.E.: 1985, *Solar Phys.* **95**, 3